

RESEARCH ARTICLE

Open Access

A reduction of viral mRNA, proteins and induction of altered morphogenesis reveals the anti-HTLV-1 activity of the labdane-diterpene myriadenolide *in vitro*

Camila Pacheco Silveira Martins^{1,2}, Orlando Abreu Gomes³, Marina Lobato Martins^{2,4}, Luciana Debortoli de Carvalho^{1,2}, Jaqueline Gontijo de Souza^{1,2}, Flavio Guimaraes Da Fonseca¹, Rodrigo Gonçalves Silva dos Santos^{1,2}, Margareth Spangler Andrade⁵, Carlos Leomar Zani⁶, Elaine Maria de Souza-Fagundes⁷ and Edel Figueiredo Barbosa-Stancioli^{1,2*}

Abstract

Background: Human T-lymphotropic virus 1 (HTLV-1) has been associated with leukemia/lymphoma (ATL) and myelopathy/tropical spastic paraparesis (HAM/TSP), in addition to other inflammatory diseases as well as infection complications. Therapeutic approaches for HTLV-1-related pathologies are limited. The labdane diterpene myriadenolide (AMY) is a natural product that exhibit biological activities, such as anti-inflammatory and antiviral activity as reported for HIV and herpesvirus.

Results: We demonstrated that this natural product was able to inhibit the expression of *gag-pol* mRNA and substantially reduced the expression of the structural proteins p19 and gp46. Comparison of treated and untreated cells shows that AMY alters both the morphology and the release of viral particles. The Atomic Force Microscopy assay showed that the AMY treatment reduced the number of particles on the cell surface by 47%.

Conclusion: We demonstrated that the labdane diterpene myriadenolide reduced the expression of the structural proteins and the budding of viral particles, besides induces altered morphogenesis of HTLV-1, conferring on AMY a new antiviral activity that may be useful for the development of new compounds with specific anti-HTLV-1 activity.

Keywords: HTLV-1, Diterpene myriadenolide, Antiviral activity, HAM/TSP, ATL

Background

Human T-lymphotropic virus 1 (HTLV-1) is the causal agent of adult T-cell leukemia (ATL), HTLV-1-associated myelopathy/tropical spastic paraparesis (HAM/TSP) and other inflammatory disorders that may develop after a variable period ranging from months to decades [1-5].

Decisions regarding ATL treatment should be based on the classification of ATL subtype, the prognostic factors at

disease onset, comorbidities and the response to initial therapy [6]. There was a successful study combining zidovudine and interferon alpha for ATL and ATL-lymphoma [7], but the most recent novelty in drugs for ATL is a promising therapeutic molecule based on a zinc finger nuclease designed to recognize and disrupt the promoter function of the HTLV-1 LTR and specifically to kill HTLV-1-infected cells, which was tested in *in vitro* and *in vivo* models [8].

Since the discovery of HAM/TSP, various therapeutic approaches have been used for patients presenting unremitting myelopathic symptoms. However, treatment is mainly symptomatic, and therapeutic guidelines for HAM/TSP are missing mainly due to the lack of randomized double-blind controlled clinical trials [9]. Because induction of chronic inflammation in the spinal

* Correspondence: edelfb@icb.ufmg.br

¹Laboratório de Virologia Básica e Aplicada (LVBA), Departamento de Microbiologia, Instituto de Ciências Biológicas, Universidade Federal de Minas Gerais, Avenida Antônio Carlos, 6627 Belo Horizonte, Minas Gerais, Brazil

²Interdisciplinary HTLV Research Group – GIPH - Fundação HEMOMINAS, Belo Horizonte, Minas Gerais, Brazil

Full list of author information is available at the end of the article

cord by HTLV-1-infected T-cells was recognized as the major pathogenic mechanism underlying HAM/TSP, anti-inflammatory and antiviral therapies have been tested [10], and some clinical benefit has been demonstrated for corticosteroids, mainly oral prednisolone and intravenous methylprednisolone [11], interferon- α [12] and IFN- β 1 [13]. In a recent study, the evaluation of the *ex vivo* and *in vitro* effects of ascorbic acid and IFN- α treatment on PBMCs of seronegative, asymptomatic carriers and HAM/TSP patients demonstrated antiproliferative and cell death-inducing and immunomodulatory effects of high-dose ascorbic acid [9].

Plants are recognized for their ability to produce a wealth of secondary metabolites, and many species have been used for centuries to treat a variety of diseases [14]. Many of these natural products have been shown to have interesting biological and pharmacological activities and are used as chemotherapeutic agents or serve as the starting point in the development of modern medicines [15-18]. *Alomia myriadenia* Schultz-Bip. ex Baker (*Asteraceae*) is an herb occurring in the central regions of Brazil. The ethanol extract of *A. myriadenia* contains the labdane-type diterpene myriadenolide (12S, 16-dihydroxy-ent-labda-7, 13-dien-15, 16-olide). Labdane-type diterpenes are known to occur in terrestrial plants and marine organisms. They display interesting biological activities, such as antibacterial, antifungal, anti-inflammatory, antileishmanial, cardiotoxic, cytotoxic and immunomodulatory activities, and show potential for use as new drugs [19-24]. Herein, we report evaluation of the antiviral potential of myriadenolide as a strategy for the development of new therapeutics to treat HTLV-1-infected patients. We show promising results for the regulation of viral messengers, expression of viral proteins, and viral morphogenesis, as evaluated with transmission electron microscopy (TEM) and atomic force microscopy (AFM).

Results

Measurement of AMY cytotoxicity

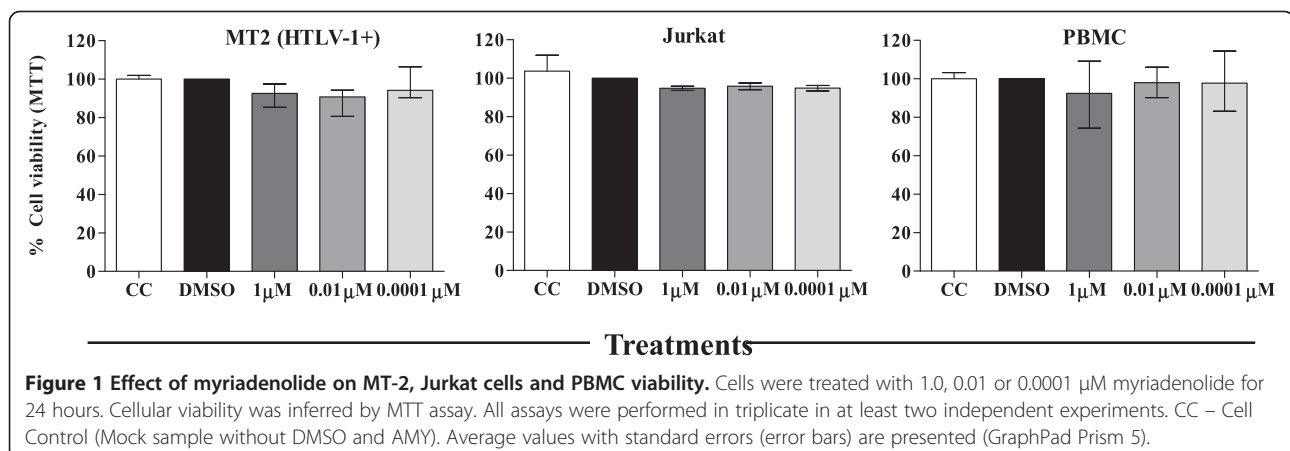
To determine AMY cytotoxicity, MT2, Jurkat cells and human PBMC were treated with 1.0, 0.01 or 0.0001 μ M AMY for 24 hours and the assay results are the mean of three independent experiments. For human PBMCs, the assay was performed in triplicate and with peripheral blood obtained from eight individuals. As demonstrated in Figure 1, treatment with different concentrations of AMY did not induce a significant reduction of cell viability in any of the cell types evaluated, compared to the diluent control (DMSO, 0.005%), showing the safety of this compound for the cell types tested, including human PBMCs, used as a control for normal cells.

Quantification of viral mRNA in MT-2 cells after treatment with AMY

The mRNA levels of the viral genes *gag-pol* (which encodes structural proteins and enzymes) and *tax-rex* (which encodes non-structural regulatory proteins) were quantified in MT-2 after 24 hours of AMY treatment using Real-Time PCR and were normalized to a cellular housekeeping gene (GAPDH). The analysis demonstrated that myriadenolide was able to inhibit the expression of *gag-pol* mRNA at 1 μ M of AMY (Figure 2). However, inhibition of *tax-rex* mRNA expression was not observed at any concentration tested.

Anti-HTLV-1 Activity of AMY in MT-2 cell line

Western blot assays were performed to determine the effect of myriadenolide on the expression level of structural protein p19 (matrix GAG protein) and gp46 (surface ENV protein) in MT-2 cells after 24 hours of AMY treatment at varying concentrations (1.0, 0.01 and 0.0001 μ M). MT-2 cells treated with AMY showed a reduction in the viral proteins tested (Figure 3a). It was interesting to observe that for matrix protein p19 and ENV protein gp46, all



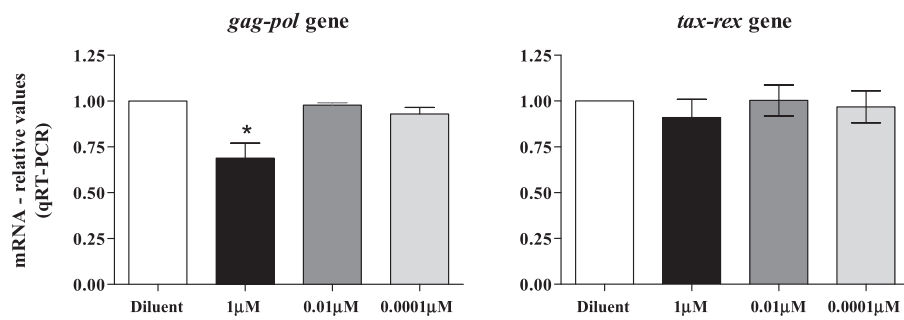
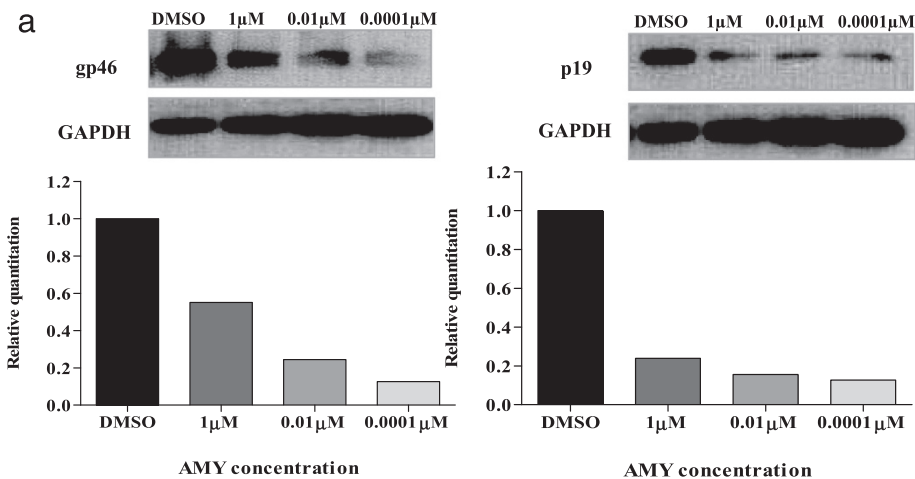


Figure 2 Effect of myriadenolide on accumulation of mRNA *gag-pol* and *tax-rex* in MT-2. Data represents the relative values of mRNA estimated by the method of relative quantification using standard curve established with cDNA from untreated MT2 cells (diluent control). Cells were treated with 1.0, 0.01 or 0.0001 μM myriadenolide for 24 hours. The assays were performed in two independent experiments. *Represents statistical difference ($p = 0.026$) between AMY 1 μM and diluent (GraphPad Prism 5; kruskall wallis with Dunn's post-test).



b Inhibitory effects of AMY on HTLV-1 protein expression in MT2 cells

	EC ₉₀ (μM)	CC ₁₀ (μM)	SI (CC ₁₀ /EC ₉₀)
gp46	0.0001	0.0288	288
p19	0.0001	0.0288	288

EC₉₀: concentration required for 90% inhibition of viral protein expression;

CC₁₀: concentration required for 10% inhibition of viability of MT-2;

SI: selectivity index (ratio of CC₁₀ to EC₉₀).

Figure 3 Expression of viral proteins is reduced in MT-2 cells treated with myriadenolide. MT-2 cells were treated with different concentrations of myriadenolide (1.0, 0.01 or 0.0001 μM) and viral protein expression was assessed. **(a)** Monoclonal primary antibodies were used to quantify protein expression: anti- gp46, p19 and GAPDH. Densitometric analysis was performed on ImageJ software to examine the level of HTLV-1 structural proteins normalized by GAPDH. **(b)** Selectivity index was calculated using CC₁₀/EC₉₀ as described in materials and methods. EC = effective concentration; CC = cytotoxic concentration.

AMY concentrations clearly decrease the level of protein expression, even at the lowest drug concentration.

In our assays, to determine the selectivity index of AMY, we choose to use the ratio CC_{10}/EC_{90} (cytotoxic concentration – cytotoxicity activity that reduced the cell viability in 10%/effective concentration - concentration that reduce the viral protein expression in 90%), as this is pharmacologically more accurate in evaluating how safe a compound is as a drug [25]. The EC_{90} value of AMY to reduce levels of gp46 and p19 was 0.0001 μ M, whereas its 10% cytotoxic concentration (CC_{10}) was 0.0228 μ M. Consequently, its selectivity index based on the ratio CC_{10}/EC_{90} was 288 (Figure 3b). These results suggest that AMY has antiviral activity interfering with the expression of structural proteins of HTLV-1.

Evaluation of AMY antiviral activity in MT-2 cells using transmission electron microscopy (TEM) and atomic force microscopy (AFM)

The TEM and AFM analyses of MT-2 cells were performed 24 h post-incubation in the presence or absence of 1 μ M AMY (Figure 4). Comparison of treated and untreated cells by TEM shows that treatment with AMY alters both the release of viral particles and the morphology (emphasized in Figure 4(b)/4(e) and 4(c)/4(f), respectively). However, we do acknowledge that the TEM may not be able to precisely determine whether these are actual complete virus particles or just empty capsids. Nonetheless, this observation was corroborated using AFM (Figure 5), and because this technique favors counting the number of particles per field evaluated, it was

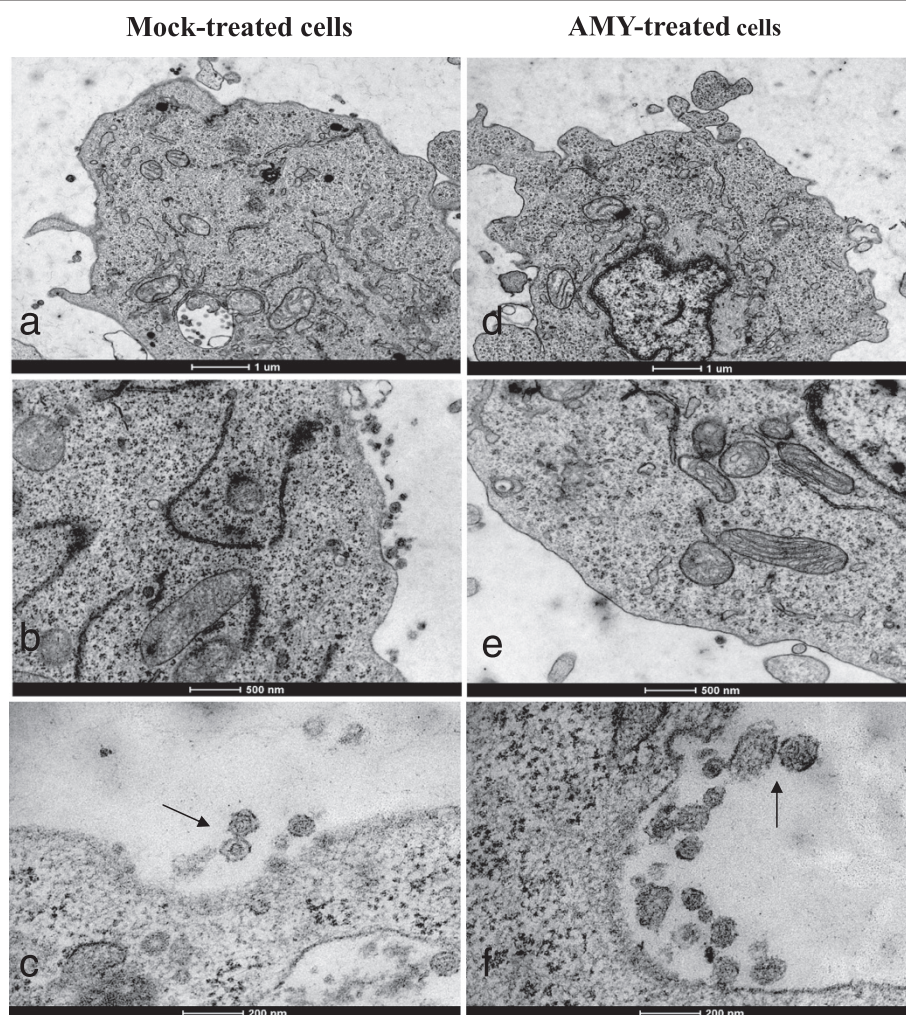


Figure 4 Transmission electron microscopy of MT-2 cells treated with AMY. MT-2 cell suspensions were cultivated with or without 1 μ M of AMY. Twenty-four hours post-incubation, cells were stained with uranyl acetate and examined under a Tecnai G² F20 electron microscope (FEI, USA). Panels **a** to **c** represent MT-2 untreated cells and **d** to **f** are MT-2 cells after AMY treatment. Viral budding is reduced in AMY treated cells when compared to mock-treated cells (panels **a**, **b**, **d** and **e**). HTLV-1 typical particles are seen when cells are untreated (panel **c**; arrow) whereas HTLV-1 atypical particles (panel **f**; arrows) are seen in AMY treated cells. Scale bars are represented in each panel.

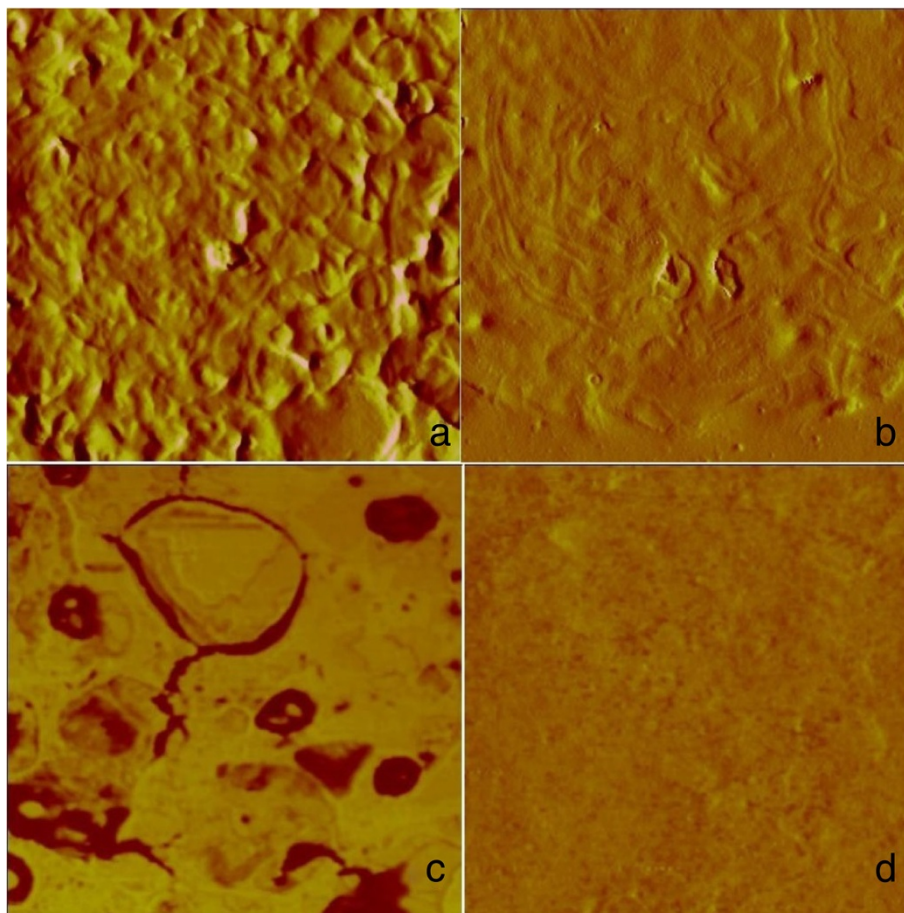


Figure 5 AFM cell surface scanning of MT2 cells treated with 1 μM and 0.001 μM AMY. The AFM images are phase and amplitude images and the regions scanned included both cells and matrix, and emphasis was placed on the cell surface. **(a)** 8.5 μm amplitude image showing the untreated MT-2 cell; **(b)** 8.5 μm image of MT-2 cell treated with 0.001 μM AMY; **(c)** 3.6 μm phase image of untreated MT-2 cells showing budding events with many virus particles embedded into a matrix; **(d)** 3.6 μm phase image of MT-2 cells treated with 1 μM AMY showing a flat cell surface with no virus budding.

shown that AMY treatment reduced the number of particles on the cell surface by 47%. Of the 412 virus particles quantified by TEM, 229 viral particles were measured in cells treated with AMY and 183 in untreated cells. In the untreated cells, the virus particles ranged from 53 to 212 nm (mean 90.6 nm), and in the treated cells, they ranged from 41 to 171 nm (mean 91.55 nm). Using AFM, a total of 158 virus particles were measured (55 and 103 particles in AMY treated and untreated cells, respectively) and the size of viruses ranged from 75.8 to 273.6 nm (mean 148.9 nm) in untreated cells, whereas the sizes ranged from 42.4 to 175.5 nm (mean 97.9 nm) in AMY treated cells.

Discussion

HTLV-1 is responsible for inducing a severe myelopathy and leukemia in humans, in addition to a number of other inflammatory pathologies for which treatment and therapeutic protocols are still ineffective. Consequently, HTLV-1 is responsible for a significant burden of morbidity and

mortality [26]. In the present study, we address the possible antiviral activity of the labdane-type diterpene myriadenolide (12*S*, 16-dihydroxy-ent-labda-7, 13-dien-15, 16-olide) for HTLV-1. The antiviral activity of the terpenes has been reported for HIV [27,28] and herpesvirus [29], among other viruses.

HTLV-1 mainly infects CD4 T cells and deregulates their differentiation, function and homeostasis, which may contribute to the pathogenesis of HTLV-1 inducing chronic inflammatory diseases [30]. HTLV gene products are engaged in dynamic activating and antagonistic interactions with host cells, mainly driven by the Tax [31] and HBZ proteins [32]. However, recent mapping of the HTLV-1 and HTLV-2 host-pathogen interactome showed that other viral proteins, including Gag and Env from both viruses, are implicated in a diverse set of cellular processes, such as the ubiquitin-proteasome system, apoptosis, multiple cancer pathways and the Notch signaling pathway [33]. Naturally infected lymphocytes produce virtually no

cell-free virions *in vivo*, and HTLV-1 is transmitted cell-to-cell through the formation of virological synapses, which are formed between an infected source cell and a susceptible target cell and play an important role in the spread of virus in the host [34]. It has also been demonstrated that there is a rapid transfer of enveloped HTLV-1 particles across virological synapses [35], reinforcing the idea that the glycoprotein Env is required for HTLV-1 infectivity [36]. Before these events, important early steps in the HTLV-1 assembly pathway include genome recognition (Gag-RNA interactions), as well as Gag-Gag and Gag-cellular protein interactions. The Gag polyprotein is composed of three domains: matrix (MA - p19), capsid (CA - p24) and nucleocapsid (NC - p15). In later steps upon budding or immediately after immature particle release, proteolytic cleavage of Gag polyproteins takes place and results in virus particle core maturation, showing that Gag coordinates assembly and viral budding [37-39]. Taken together, this information about morphogenesis, viral spread and virus-cell regulation introduces new concepts to target drugs for HTLV-1.

In this context, our results first revealed that the myriadenolide compound was able to reduce the accumulation of *gag-pol* mRNA at 1 μ M after 24 hours of treatment (although no variation was seen for *tax-rex* mRNA in any concentration tested). HTLV-1 requires regulated gene expression from unspliced and alternatively spliced transcripts for efficient replication and persistence, being able to export intron-containing mRNAs to cytoplasm for subsequent translation, function related to the viral protein Rex [40]. Rex phosphoprotein acts posttranscriptionally by preferentially binding, stabilizing, and selectively exporting the unspliced and incompletely spliced viral mRNA from the nucleus to the cytoplasm, essentially regulating production of the virion components [41]. Experiments conducted with transient transfection of 293T cells with the HTLV-1 plasmid, as well as newly HTLV-1 infected human PBMCs, clarified that incompletely spliced (*env*) and doubly spliced transcripts (*tax/rex*) are not generated at the same rate from full-length transcripts (*gag-pol*) [42]. Other important point is that unlike the *gag/pol* and *env* transcripts encoding the structural and enzymatic proteins, the efficient expression and cytoplasmic export of the alternatively spliced regulatory and accessory transcripts are not directly dependent on Rex [40]. However, the exact mechanism supporting the distinct activity observed upon AMY treatment for *gag-pol* and *tax-rex* transcripts remains to be determined. Nonetheless, we could speculate that phenomenon is based on differential gene expression regulation and Rex dependence for stability and transport of the both transcripts.

We observed a significant reduction on p19 and gp46 protein expression when using three different AMY concentrations (1.0, 0.01 and 0.0001 μ M). Curiously the

decreasing concentrations of AMY have increasing inhibitory activity on HTLV-1 antigen expression in MT2 cells (Figure 3a). This represents the hormetic dose-response effect (hormesis), in which a low dose can define the therapeutic zone (the intended effect, in our case, antiviral properties). Hormesis is a dose response relationship in which effects at low doses are opposite to those at high doses. Recent relevant reports analyzing hormetic dose responses indicates that this phenomenon can have specific mechanisms mediated by different receptors and signaling pathways, having biological diverse effects in distinct doses [43-45]. Thus, hormesis could explain why the lowest concentration of AMY (0.0001 μ M) was best at reducing viral protein expression. Nonetheless, we did not see the same effect when analyzing transcript levels for the same proteins. At this point we still do not have a verifiable explanation to this otherwise biological effect.

The results also emphasize that AMY demonstrated no cytotoxicity when evaluated at concentrations up to 1 μ M, as previously described by our group [24]. The selectivity index (288) showed that reduction of viral protein expression occurs with low toxicity. In drug discovery, it is desirable to have a high therapeutic/selectivity index (i.e., maximum antiviral activity with minimal cell toxicity). An index higher than 50 is considered as indicative of highly active compounds [46].

In concert with TEM, which clearly showed differences in particle morphology in treated and untreated cells (Figure 4), we used scanning AFM in air tapping mode to obtain more reliable results for viral particle measurement and number of budding particles. For untreated cells, the viruses ranged from 75.8 to 273.6 nm (mean 148.9 nm), and in treated cells, they ranged from 42.4 to 175.5 nm (mean 97.9 nm). Experiments using TEM and AFM proved that treatment of MT-2 for 24 hours using 1.0 μ M myriadenolide was able to reduce the amount of virus at the cell surface (approximately 47%) and to modify the morphogenesis of viral particles, in accordance with the protein inhibition observed in Western blot assays.

Conclusions

These results showed promising anti-HTLV-1 activity, mainly inhibition of Gag and Env protein expression and interference in viral budding and morphogenesis. It may be hypothesized that disruption in viral replication functions could reduce viral spread in infected hosts, suggesting a potential for AMY to be used as an anti-HTLV-1 therapeutic drug.

Methods

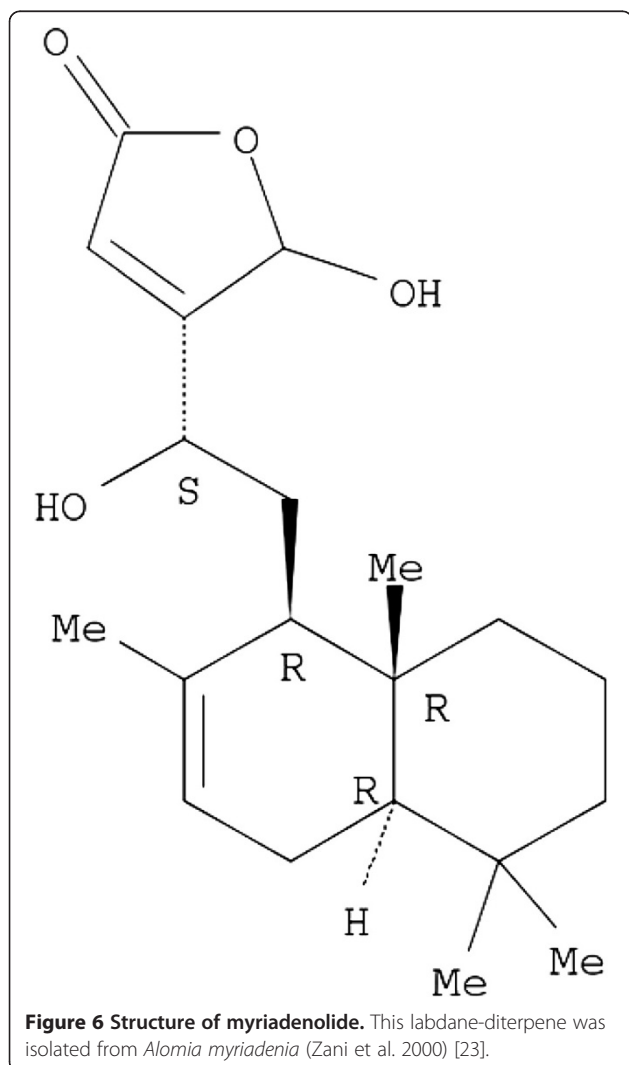
Cells

In this study, MT-2, an HTLV-1-infected T-cell line, and uninfected Jurkat T-cells were used. For the viability

assays, human peripheral blood mononuclear cells (PBMCs) from seronegative blood donors were also used. Written informed consent was obtained, and this study was approved by the Ethics Committee of UFMG and Fundação HEMOMINAS. The cells were maintained in RPMI-1640 medium supplemented with 10-20% v/v fetal bovine serum (Life Technologies), 2 mM L-glutamine, 100 U penicillin mL⁻¹ and 50 µg gentamicin mL⁻¹ (SIGMA-ALDRICH).

Myriadenolide

Myriadenolide (AMY, Figure 6) was isolated from an ethanol extract of aerial parts of *Alomia myriadenia* Schultz-Bip. Ex. Baker (*Asteraceae*) (voucher code BHCB 42865) as previously described [23]. The AMY compound was dissolved in DMSO, diluted in RPMI and added to the culture to attain the desired final concentrations. Control experiments were performed using DMSO (0.005%).



Cellular viability (MTT assay)

The cytotoxicity was determined in parallel with the antiviral activity. For that, cell viability was estimated measuring the rate of mitochondrial reduction of yellow tetrazolium salt MTT (3-(4,5-dimethylthiazol-2-yl)-2,5-diphenyltetrazolium bromide; Sigma-Aldrich, St. Louis, MO) to insoluble purple crystals [47]. After AMY incubation, MTT solution (20 µL; 5 mg MTT mL⁻¹) was added to each well and incubated for 4 hours. At the end of this incubation, the supernatant was removed and 200 µL of 0.04 M HCl in isopropyl alcohol were added to dissolve the formazan crystal. The optical densities (OD) were measured with a spectrophotometer at 590 nm. Results were normalized with DMSO control (0.005%) and expressed as percentage of cell viability. Data were analyzed using Prism 5.0 (GraphPad Software Inc.).

The EC₉₀ was determined as the concentration to reduce the viral protein expression in 90% using densitometry (measurement of the density of the viral protein bands in Western blot assay comparing with the mock treated cell [diluent control - DMSO 0.005%]) by the equation: % reduction of viral protein = 100 - (Densitometry values of treated cells × 100) / densitometry values of the control). The CC₁₀ was defined as the cytotoxic activity that reduced the cell viability in 10%, and was measured comparing the treated cell with the mock treated cell. The equation used was: % reduction of viability = 100 - (Absorbance of treated cells × 100) / Absorbance of mock treated cell. The concentrations needed to achieve 90% of reduction of viral protein expression, i.e., effective concentration (EC₉₀), as well as the concentration needed to cause 10% cytotoxicity, i.e., cytotoxic concentration (CC₁₀) was determinate as described [25]. Antiviral indices or selectivity index (SI) were then calculated as CC₁₀/EC₉₀.

Quantification of *gag-pol* and *tax-rex* mRNA expression

RNA was extracted from MT-2 cells using Trizol (Life Technologies, Carlsbad, CA, USA), and complementary DNA was synthesized from 1 µg RNA using the High-Capacity cDNA Reverse Transcription Kit with random primers (Applied Biosystems, Foster City, USA), according to the manufacturer's instructions. Expression levels of *gag-pol* and *tax-rex* mRNA were quantified using real-time PCR with serially diluted cDNA (250, 25, 2.5 and 0.25 ng) from HTLV-1-infected MT-2 cells to generate standard curves, and *GAPDH* was used as a reference gene. The amplification reaction for each gene (in separate tubes) was performed using cDNA synthesized from 250 ng RNA and 1X SYBR Green PCR Master Mix (Applied Biosystems, Foster City, CA, USA) in a final volume of 25 µL with 5 pM of the following primers according to Li & Green [48]: 5'- ACCAACACCAT GGCCA -3' (sense) and 5'- GAGTCGAGGGATAA

GGAAC -3' (antisense) for *tax-rex*; 5'- GAGGGAGG AGCAAAGGTACTG -3' (sense) and 5'- AGCCCCCA GTTCATGCAGACC -3' (antisense) for *gag-pol*; and 5'- ACAGTCAGCCGCATCTTCTT -3' (sense) and 5'- AC GACCAAATCCGTTGACTC -3' (antisense) for human *GAPDH* (NM_002046.2). Real-time PCR was performed in an ABI Prism 7300 Sequence Detector System (Applied Biosystems, Foster City, CA, USA) with the following cycle conditions: 2 min at 50°C and 10 min at 95°C, followed by 45 cycles of 15 s at 95°C and 1 min at 60°C. Melting curves were performed after the end of the amplification cycles to validate the specificity of the amplified products. All standard dilutions and the control and individual samples were run in triplicate. Quantification was accepted when standard curves had slopes between -3.10 and -3.74, and the r^2 was >0.99. The expression of *gag-pol* and *tax-rex* mRNA was calculated using the value of the target gene/value of *GAPDH*.

Antiviral activity (viral protein reduction by immunoblotting assay)

The antiviral potential of AMY against HTLV-1 was based on the inhibition of p19 and gp46 viral proteins in permanently infected MT-2 cells by immunoblotting analysis. Briefly, MT-2 cells were treated in the absence (0.05% DMSO) or presence of AMY for 24 hours (1.0, 0.01 or 0.0001 μ M). Cell extracts were prepared using lysis buffer (50 mM Tris-HCl, pH 7.4, 150 mM sodium chloride, 50 mM sodium fluoride, 10 mM beta-glycerophosphate, 0.1 mM ethylenediaminetetraacetic acid, 10% glycerol, 1% Triton X-100, 1 mM phenylmethylsulfonyl fluoride, 2 mM sodium orthovanadate and 2 mg/ml each of pepstatin, leupeptin and aprotinin). Following incubation on ice for 10 min, cell extracts were clarified by centrifugation at 10,000 *g* for 20 min. Proteins were assayed using the Bradford reagent (Bio-Rad, Hercules), and 40 μ g of extract from each sample was resolved by SDS-PAGE and transferred to nitrocellulose membranes (Bio-Rad Laboratories). Blots were evaluated using primary anti-HTLV-1 antibodies (monoclonal anti-p19: sc-57868; anti-gp46: sc-57865 and anti-GAPDH: sc-66163 from Santa Cruz Biotechnology), and after incubation with secondary antibody, immunoreactive bands were detected by enhanced chemiluminescence according to the manufacturer's instructions (GE Healthcare). Densitometric analysis was performed on ImageJ software.

Transmission electron microscopy (TEM)

MT-2 cell suspensions containing 10^6 cells/well were cultivated with or without 1 μ M AMY. Twenty-four hours post-incubation, cells were harvested by centrifugation at 400 *g* for 5 min at 4°C and washed twice with RPMI. Cells were collected and fixed in 2.5% glutaraldehyde for 18 hours. After washes in 0.1 M sodium cacodylate, fixed

samples were post-fixed in 1% osmium tetroxide for 30 min. Samples were dehydrated in a graded acetone series prior to infiltration and embedding (Epon 812 resin). Ultrathin longitudinal sections (65 nm) were cut, stained with uranyl acetate and lead citrate and examined under a Tecnai G² F20 electron microscope (FEI).

Atomic force microscopy (AFM) scanning

AFM imaging was performed at room temperature on equipment monitored by a NanoScope IIIa controller from Bruker AXS (Santa Barbara) operated in tapping mode and equipped with phase-imaging hardware. Commercial tapping mode tips from MikroMasch (Sofia) with 230- μ m-long cantilevers, resonance frequencies of 60–90 kHz, spring constants of 2.0–5.0 N/m and a nominal tip curvature radius of 10 nm were used. Prior to microscopy, 13-mm round glass slides were washed exhaustively with neutral detergent and incubated in distilled water at 60°C overnight to remove the remaining dirt and grease. The glass slides were rinsed again with cold Milli Q water and subsequently rinsed with 100% ethanol and dried under laminar flow. After drying, 500 μ l 1% poly-L-lysine was added to the slides (SIGMA-ALDRICH), and the slides were dried again under laminar flow. Cleaved mica (Ted Pella Inc) was also used for cell analysis. MT-2 cells treated with or without 1 μ M and 0.001 μ M AMY were centrifuged in a cytospin centrifugation apparatus (Jouan) (1000 *g*, 10 min, 4°C; 5.0×10^5 cells) onto the glass slide or cleaved mica. After centrifugation, the cells were dehydrated successively with 30%, 50% and 70% ethanol. The slides were then fixed with cold methanol and dried under laminar flow. The AFM images presented here are phase and amplitude images. The sizes and heights of structures indicating HTLV-1 on the surface and viral budding were measured in 5 fields by glass slide or cleaved mica using the NanoScope software and Gwyddion software (<http://gwyddion.net/>) [49].

Ethics statement

This study was conducted as an in-vitro study using cell lines. However, human PBMC was used as a control in the cell viability test and written informed consent was obtained, and this study was approved by the Ethics Committee of UFMG and Fundação HEMOMINAS.

Abbreviations

HTLV-1: Human T-lymphotropic virus 1; ATL: Adult T-cell leukemia; HAM/TSP: HTLV-1-associated myelopathy/tropical spastic paraparesis; AMY: Labdane diterpene myriadenolide; TEM: Transmission electron microscopy; AFM: Atomic force microscopy.

Competing interests

The authors declare that they have no competing interests.

Authors' contributions

CPSM, JGS, RGSS and LDC carried out the experimental procedures; OAG, FGDF and MSA contributed with the Atomic Force Microscopy experiments;

CLZ isolated and prepared the Myriadenolide; EMSF, MLM, FGDF and EFBS designed the study and contributed equally to the analysis and production of the final manuscript. All authors read and approved the final manuscript.

Acknowledgments

Financial support was provided by Fundação de Amparo à Pesquisa de Minas Gerais (FAPEMIG), Conselho Nacional de Desenvolvimento Científico e Tecnológico (CNPq), Coordenação de Aperfeiçoamento de Pessoal de Nível Superior (CAPES) and Pro-Reitoria de Pesquisa da UFMG (PRPq). E.F. Barbosa-Stancioli, F.G. Da Fonseca, J.G. Souza, L.D. Carvalho and C.P.S. Martins received fellowships from CNPq. The authors also thank the Fundação HEMOMINAS and Dr. Anna Barbara Carneiro-Proietti for supporting the Interdisciplinary HTLV Research Group (GIPH), which has contributed steadily to research on HTLV.

Author details

¹Laboratório de Virologia Básica e Aplicada (LVBA), Departamento de Microbiologia, Instituto de Ciências Biológicas, Universidade Federal de Minas Gerais, Avenida Antônio Carlos, 6627 Belo Horizonte, Minas Gerais, Brazil. ²Interdisciplinary HTLV Research Group – GIPH - Fundação HEMOMINAS, Belo Horizonte, Minas Gerais, Brazil. ³Núcleo de Ciências Exatas – FACE – Universidade FUMEC, Belo Horizonte, Minas Gerais, Brazil. ⁴Serviço de Pesquisa, Fundação HEMOMINAS, Belo Horizonte, Minas Gerais, Brazil. ⁵Centro Tecnológico SENAI CETEC, Belo Horizonte, Minas Gerais, Brazil. ⁶Centro de Pesquisas René Rachou, FIOCRUZ, Belo Horizonte, Minas Gerais, Brazil. ⁷Departamento de Fisiologia e Biofísica, Instituto de Ciências Biológicas, Universidade Federal de Minas Gerais, Belo Horizonte, Minas Gerais, Brazil.

Received: 2 July 2014 Accepted: 17 December 2014

Published online: 24 December 2014

References

- Yoshida M, Miyoshi I, Hinuma Y: Isolation and characterization of retrovirus from cell lines of human adult T-cell leukemia and its implication in the disease. *Proc Natl Acad Sci* 1982, **79**:2031–2035.
- Osame M, Usuku K, Izumo S, Ijichi N, Amitani H, Igata A, Matsumoto M, Tara M: HTLV-I associated myelopathy, a new clinical entity. *Lancet* 1986, **1**:1031–1032.
- Watanabe T: HTLV-1-associated diseases. *Int J Hematol* 1997, **66**:257–278.
- Gout O, Baulac M, Gessain A, Semah F, Saal F, Périès J: Rapid development of myelopathy after HTLV-1 infection acquired by transfusion during cardiac transplantation. *N Engl J Med* 1990, **322**:383–388.
- Gillet N, Carpentier A, Barez PY, Willems L: WIP1 deficiency inhibits HTLV-1 Tax oncogenesis: novel therapeutic prospects for treatment of ATL? *Retrovirology* 2012, **9**:115.
- Tsukasaki K, Hermine O, Bazarbachi A, Ratner L, Ramos JC, Harrington W Jr, O'Mahony D, Janik JE, Bittencourt AL, Taylor GP, Yamaguchi K, Utsunomiya A, Tobinai K, Watanabe T: Definition, prognostic factors, treatment, and response criteria of adult T-cell leukemia-lymphoma: a proposal from an international consensus meeting. *J Clin Oncol* 2009, **27**:453–459.
- Bazarbachi A, Hermine O: Treatment with a combination of zidovudine and alpha-interferon in naive and pretreated adult T-cell leukemia/lymphoma patients. *J Acquir Immune Defic Syndr Hum Retrovirol* 1996, **13**(Suppl 1):186–190.
- Tanaka A, Takeda S, Kariya R, Matsuda K, Urano E, Okada S, Komano J: A novel therapeutic molecule against HTLV-1 infection targeting provirus. *Leukemia* 2013, **27**:1621–1627.
- Moens B, Decanine D, Menezes SM, Khouri R, Silva-Santos G, Lopez G, Alvarez C, Taliedo M, Gotuzzo E, de Almeida KR, Galvão-Castro B, Vandamme AM, Van Weyenbergh J: Ascorbic acid has superior ex vivo antiproliferative, cell death-inducing and immunomodulatory effects over IFN- α in HTLV-1-associated myelopathy. *PLoS Negl Trop Dis* 2012, **6**:e1729.
- Yamano Y, Sato T: Clinical pathophysiology of human T-lymphotropic virus-type 1-associated myelopathy/tropical spastic paraparesis. *Front Microbiol* 2012, **3**:389.
- Nakagawa M, Nakahara K, Maruyama Y, Kawabata M, Higuchi I, Kubota H, Izumo S, Arimura K, Osame M: Therapeutic trials in 200 patients with HTLV-I-associated myelopathy/tropical spastic paraparesis. *J Neurovirol* 1996, **2**:345–355.
- Izumo S, Goto I, Itoyama Y, Okajima T, Watanabe S, Kuroda Y, Araki S, Mori M, Nagataki S, Matsukura S, Akamine T, Nakagawa M, Yamamoto I, Osame M: Interferon-alpha is effective in HTLV-I-associated myelopathy: a multicenter, randomized, double-blind, controlled trial. *Neurology* 1996, **46**:1016–1021.
- Oh U, Yamano Y, Mora CA, Ohayon J, Bagnato F, Butman JA, Dambrosia J, Leist TP, McFarland H, Jacobson S: Interferon-b1a therapy in human T-lymphotropic virus type I-associated neurologic disease. *Ann Neurol* 2005, **57**:526–534.
- Cragg GM, Boyd MR, Khanna R, Kneller R, Mays TD, Mazan KD, Newman DJ, Sausville EA: International collaboration in drug discovery and development: the NCI experience. *Pure Appl Chem* 1999, **71**:1619–1633.
- Verpoorte R: Exploration of nature's chemodiversity: the role of secondary metabolites as leads in drug development. *Drug Develop Trends* 1988, **3**:232–238.
- Verpoorte R: Pharmacognosy in the new millennium: leadfinding and biotechnology. *J Pharm Pharmacol* 2000, **52**:253–262.
- Balunas MJ, Kinghorn AD: Drug discovery from medicinal plants. *Life Sci* 2005, **78**:431–441.
- Sadqui M, Fushman D, Munoz V: Atom-by-atom analysis of global downhill protein folding. *Nature* 2006, **442**:317–321.
- Fernandez MA, Tornos MP, Garcia MD, de las Heras B, Villar AM, Saenz MT: Anti-inflammatory activity of abietic acid, a diterpene isolated from *Pimenta racemosa* var. *grisea*. *J Pharm Pharm Sci* 2001, **53**:867–872.
- Navarro A, de las Heras B, Villar A: Immunomodulating properties of diterpene andalusol. *Planta Med* 2000, **66**:289–291.
- Singh M, Pal M, Sharma RP: Biological activity of the labdane diterpenes. *Planta Med* 1999, **65**:2–8.
- Dimas K, Demetzos C, Marsellos M, Sotiriadou R, Malamas M, Kokkinopoulos D: Cytotoxic activity of labdane type diterpenes against human leukemia cell lines in vitro. *Planta Med* 1998, **64**:208–211.
- Zani C, Alves TMA, Queiroz R, Fontes ES, Shin YG, Cordell GA: A cytotoxic diterpene from *Alomia myriadenia*. *Phytochem* 2000, **53**:877–880.
- Souza-Fagundes EM, Gazzinelli G, Parreira GG, Martins-Filho AO, Amarante-Mendes GP, Correa-Oliveira R, Zani CL: In vitro activity of labdane diterpene from *Alomia myriadenia* (Asteraceae): immunosuppression via induction of apoptosis in monocytes. *Int Immunopharmacol* 2003, **3**:383–392.
- Ayisi NK, Gupta SV, Qualtiere LF: Modified tetrazolium-based calorimetric method for determining the activities of anti-HIV compounds. *J Virol Methods* 1991, **33**:335–344.
- Cook LB, Elemans M, Rowan AG, Asquith B: HTLV-1: persistence and pathogenesis. *Virology* 2013, **435**:131–140.
- Ohyoshi T, Funakubo S, Miyazawa Y, Niida K, Hayakawa I, Kigoshi H: Total synthesis of (-)-13-oxingenol and its natural derivative. *Angew Chem Int Ed Engl* 2012, **51**:4972–4975.
- Pan LL, Fang PL, Zhang XJ, Ni W, Li L, Yang LM, Chen CX, Zheng YT, Li CT, Hao XJ, Liu HY: Tiglane-type diterpenoid glycosides from *Euphorbia fischeriana*. *J Nat Prod* 2011, **74**:1508–1512.
- Khan MT, Ather A, Thompson KD, Gambari R: Extracts and molecules from medicinal plants against herpes simplex viruses. *Antiviral Res* 2005, **67**:107–119.
- Satou Y, Matsuoka M: Virological and immunological mechanisms in the pathogenesis of human T-cell leukemia virus type 1. *Rev Med Virol* 2013, **5**:269–280.
- Boxus M, Twizere JC, Legros S, Dewulf JF, Kettmann R, Willems L: The HTLV-1 Tax interactome. *Retrovirology* 2008, **5**:76.
- Satou Y, Matsuoka M: Molecular and Cellular Mechanism of Leukemogenesis of ATL: Emergent Evidence of a Significant Role for HBZ in HTLV-1-Induced Pathogenesis. *Leuk Res Treatment* 2012, **21**:3653.
- Simonis N, Rual JF, Lemmens I, Boxus M, Hirozane-Kishikawa T, Gatot JS, Dricot A, Hao T, Vertommen D, Legros S, Daakour S, Klitgord N, Martin M, Willaert JF, Dequiedt F, Navratil V, Cusick ME, Burny A, Van Lint C, Hill DE, Tavernier J, Kettmann R, Vidal M, Twizere JC: Host-pathogen interactome mapping for HTLV-1 and -2 retroviruses. *Retrovirology* 2012, **9**:26.
- Igakura T, Stinchcombe JC, Goon PK, Taylor GP, Weber JN, Griffiths GM, Tanaka Y, Osame M, Bangham CR: Spread of HTLV-I between lymphocytes by virus-induced polarization of the cytoskeleton. *Science* 2003, **299**:1713–1716.
- Majorovits E, Nejmeddine M, Tanaka Y, Taylor GP, Fuller SD, Bangham CR: Human T-lymphotropic virus-1 visualized at the virological synapse by electron tomography. *PLoS One* 2008, **3**:e2251.
- Delamarre L, Pique C, Rosenberg AR, Blot V, Grange MP, Le Blanc I, Dokh elar MC: The Y-S-L-I tyrosine-based motif in the cytoplasmic domain of the human

- T-cell leukemia virus type 1 envelope is essential for cell-to-cell transmission. *J Virol* 1999, **73**:9659–9663.
37. Le Blanc I, Blot V, Bouchaert I, Salamero J, Goud B, Rosenberg AR, Dokh elar MC: **Intracellular distribution of human T-cell leukemia virus type 1 Gag proteins is independent of interaction with intracellular membranes.** *J Virol* 2002, **76**:905–911.
 38. Grigsby IF, Zhang W, Johnson JL, Fogarty KH, Chen Y, Rawson JM, Crosby AJ, Mueller JD, Mansky LM: **Biophysical analysis of HTLV-1 particles reveals novel insights into particle morphology and Gag stoichiometry.** *Retrovirology* 2010, **7**:75.
 39. Fogarty KH, Zhang W, Grigsby IF, Johnson JL, Chen Y, Mueller JD, Mansky M: **New insights into HTLV-1 particle structure, assembly, and Gag-Gag interactions in living cells.** *Viruses* 2011, **3**:770–793.
 40. Li M, Kannian P, Yin H, Kesic M, Green PL: **Human T lymphotropic virus type 1 regulatory and accessory gene transcript expression and export are not rex dependent.** *AIDS Res Hum Retroviruses* 2012, **28**:405–410.
 41. Younis I, Khair L, Dundr M, Lairmore MD, Franchini G, Green PL: **Repression of human T-cell leukemia virus type 1 and type 2 replication by a viral mRNA-encoded posttranscriptional regulator.** *J Virol* 2004, **78**:11077–11083.
 42. Li M, Kesic M, Yin H, Yu L, Green PL: **Kinetic analysis of human T-cell leukemia virus type 1 gene expression in cell culture and infected animals.** *J Virol* 2009, **83**:3788–3797.
 43. Calabrese EJ: **Hormetic mechanisms.** *Crit Rev Toxicol* 2013, **43**:580–606.
 44. Calabrese EJ: **Hormesis: from mainstream to therapy.** *J Cell Commun Signal.* 2014. Nov 1. [Epub ahead of print] PubMed PMID: 25366126.
 45. Cornelius C, Koverech G, Crupi R, Di Paola R, Koverech A, Lodato F, Scuto M, B Salinaro AT, Cuzzocrea S, Calabrese EJ, Calabrese V: **Osteoporosis and alzheimerpathology: role of cellular stress response and hormetic redox signaling in aging and bone remodeling.** *Front Pharmacol* 2014, **10**:120.
 46. Severson W, McDowell M, Ananthan S, Chung DH, Rasmussen L, Sosa MI, White LE, Noah J, Colleen B: **High-throughput screening of a 100,000 compound library for inhibitors of influenza A virus (H3N2).** *J Biomol Screen* 2008, **13**:879–887.
 47. Mosmann T: **Rapid colorimetric assay for cellular growth and survival: application to proliferation and cytotoxicity assays.** *J Immunol Methods* 1983, **65**:55–63.
 48. Li M, Green PL: **Detection and quantification of HTLV-1 and HTLV-2 mRNA species by real-time RT-PCR.** *J Virol Methods* 2007, **142**:159–168.
 49. Coelho-dos-Reis JG, Martins-Filho OA, de Brito-Melo GE, Gallego S, Carneiro-Proietti AB, Souza JG, GIPH, Barbosa-Stancioli EF: **Performance of IgG and IgG1 anti-HTLV-1 reactivity by an indirect immunofluorescence flow cytometric assay for the identification of persons infected with HTLV-1, asymptomatic carriers and patients with myelopathy.** *J Virol Methods* 2009, **160**(1–2):138–148.

Submit your next manuscript to BioMed Central and take full advantage of:

- Convenient online submission
- Thorough peer review
- No space constraints or color figure charges
- Immediate publication on acceptance
- Inclusion in PubMed, CAS, Scopus and Google Scholar
- Research which is freely available for redistribution

Submit your manuscript at
www.biomedcentral.com/submit

